STAR FORMATION DENSITY AND GALACTIC OUTFLOWS AT z∼2

by

Matthew Coon

A Thesis Submitted in

Partial Fulfillment of the

Requirements for the Degree of

Master of Science

in Physics

at

The University of Wisconsin-Milwaukee

December 2017

ABSTRACT

STAR FORMATION DENSITY AND GALACTIC OUTFLOWS AT z∼2

by

Matthew Coon

The University of Wisconsin-Milwaukee, 2017
Under the Supervision of Professor Dawn K. Erb

Galactic-scale outflows of gas play a significant role in galaxy evolution. They push gas to larger radii, slowing the star formation rate near the center of the galaxy, and increasing it at larger radii. Eventually, these outflows can expel the gas from the galaxy, depositing metals into the intergalactic medium, and limiting star formation in the galaxy. Galaxies from the Keck Baryonic Structure Survey (KBSS) and 3D-Hubble Space Telescope (3D-HST) Survey were used in order to measure the velocities of galactic outflows from the KBSS spectra, and the grism spectra from the 3D-HST survey were used in order to map the sizes of star forming regions based on emission lines. These galaxies were filtered such that only galaxies with prominent [OIII] $\lambda\lambda$4959, 5007 doublet emissions and whose outflow velocities could be calculated were kept. After the filter, 52 galaxies remained. Local galaxies with high surface densities of star formation are known to have stronger galactic outflows. To test if this is true at z∼2, the [OIII] luminosity surface density was used as an analog to the SFR, and it was compared to the outflow velocity in each galaxy. A correlation significance of 0.4σ was found, indicating no correlation between the two values. This disagrees with some existing results. The lack of correlation could be due to a lack of range in galaxy properties. It is recommended to use Hα emission to more directly measure the star formation rates in the future, instead of using [OIII] as an analog to the SFR.

TABLE OF CONTENTS

LIST OF FIGURES

ACKNOWLEDGEMENTS

This work is based on observations with the NASA/ESA Hubble Space Telescope, which is operated by the Association of Universities for Research in Astronomy, Inc., under NASA contract NAS5-26555. This work is also based on data obtained at the W. M. Keck Observatory, which is operated as a scientific partnership among the California Institute of Technology, The University of California, and NASA, and was made possible by the generous financial support of the W. M. Keck Foundation. A further thanks to those of Hawaiian ancestry, on whose sacred mountain these data were obtained. An additional thank you to Gabriel Brammer, for allowing use of his Grizli Reduction and his willingness to assist in the use of his program. Finally, I would like to thank my advisor Dawn Erb, for giving me the opportunity to work on this project, for her generous assistance and patience during its completion, and for her feedback throughout the process.

Chapter 1

Introduction

It has been well established that galactic-scale outflows of gas are present in almost all starburst galaxies in the local universe (Heckman, 2002), and nearly all star-forming galaxies at higher redshifts (Shapley, 2011; Steidel et al., 2010). These outflows are also known to play an important role in star formation feedback loops (Murray et al., 2005). Outflows take gas away from actively star-forming regions, causing star formation there to slow. In the process, it brings the gas further outward, allowing stars to form at larger radii (Nelson et al., 2012; Nelson et al., 2016). Eventually, these outflows can remove the gas from the galaxy, and deposit it in the intergalactic medium (Heckman, 2002; Steidel et al., 2010). Finding relations between these outflows and properties of their host galaxies can provide valuable insight into galaxy evolution.

1.1 Outflows and galaxy evolution

Outflows are often invoked to explain various aspects of galactic evolution. They can explain the inside out growth of galaxies (Nelson et al., 2012; Nelson et al., 2016) and why a galaxy ceases major star formation (Murray et al., 2005). They also provide a possible explanation as to why metals, which come from stars, exist in the intergalactic medium (IGM) (Heckman, 2002; Steidel et al., 2010), where stars are

seldom present.

To properly discuss outflows, we must first define what they are. Heckman (2002) states that starburst-driven galactic winds are "complex multiphase outflows of cool, warm, and hot gas, dust, and magnetized relativistic plasma." These winds can have a range of velocities from $\sim 10^2 - 10^3$ km/s. He also states that winds are nearly always present in galaxies with a global star formation rate per unit area of over $0.1 M_\odot$ yr^{-1} kpc^{-2}, which local starburst galaxies and nearly all high redshift galaxies achieve. This value is higher than the value of $0.05 M_\odot$ yr^{-1} kpc^{-2} obtained by Murray et al. (2011) for the critical surface density of star formation rate required to drive galactic outflows.

There are multiple methods of generating these winds. It has been shown (Chevalier & Clegg, 1985) that if energy from a supernova is thermalized, it can create a strong wind capable of expelling gas from a region. However, a single mechanism cannot produce the winds that we observe around starburst galaxies (Hopkins et al., 2012). Supernovae are capable of driving hot winds, but this process alone quickly destroys any cold winds that would be present (Murray et al., 2011). Therefore, another driving mechanism must exist since we are able to observe cool winds. Radiation pressure from hot, young stars is able to produce winds that can drive gas out of the disk of the galaxy and preserve the cool winds that are observed.

With gaseous outflows, the gas will be transported from the center of the galaxy, outwards (Chevalier & Clegg, 1985). This movement of gases causes the star formation rate to slow in the inner regions, while it increases at larger radii (Nelson et al., 2012; Nelson et al., 2016). Nelson et al. (2016) looked at 3200 galaxies from $0.7 < z < 1.5$ and found that the active star forming regions of a galaxy were generally near its edges. This outflow of gas causes the active star forming regions to move towards larger radii.

Eventually however, this star formation stops. Murray et al. (2005) found that

galaxies have a limiting, Eddington-like luminosity, that when reached, would expel much of the surrounding gas from the galaxy. This expulsion would starve a galaxy of gas and cause most major star formation to cease.

1.2 Correlations of outflows and galaxy properties

Previous studies have also tried to determine the drivers of galactic outflows by finding properties of galaxies that appear to correlate with the outflow velocity. The absorption line velocity shift is determined based on the systemic redshift of the galaxy, and the redshift of the interstellar gas seen via absorption lines. The systemic redshift is the redshift of the stars in the galaxy, and is determined by the nebular emission lines from ionized gas around the more massive stars. However, the stellar continuum light also interacts with the gas in the galaxy and creates absorption lines that can be observed in the spectrum. If this gas is moving, and in the foreground of the galaxy, the doppler shift relative to the host galaxy will cause the absorption lines to have a relative blueshift from the host galaxy. By examining both of these redshifts, the outflow velocity can be determined.

After the outflow velocity is determined, it can be compared to other properties of the galaxy to determine if they are correlated. One such example of this is given by Martin (2005), who found that the winds in more luminous starburst galaxies accelerate gas to higher speeds roughly as $v \propto SFR^{0.35}$, where SFR is the star formation rate.

Heckman et al. (2015) found multiple correlations between outflow velocity and properties of the host galaxy. They found that outflow velocity (v_{out}) correlates weakly with galaxy stellar mass and the galaxy's circular velocity around its center (v_{cir}). On the other hand, v_{out} was found to correlate strongly with both SFR and SFR/area. Additionally v_{out}/v_{cir} was found to correlate strongly with SFR/area and SFR/M_*,

where M_* is the stellar mass in the galaxy. However, it was found that v_{out} does not correlate with $\dot{M}$/SFR, where $\dot{M}$ is the mass outflow rate. Using these results, they continue on to show that these results imply an outflow model that consists of momentum-driven clouds of gas, rather than a momentum-driven shell of gas.

Heckman et al. (2015) found that the outflows removed gas at an estimated rate ($\dot{M}$) that is $1-4$ times higher than the SFR. In addition, Hopkins et al. (2012) found that the outflow rates can be as high as $\sim 10-20$ times the SFR.

1.3 Star-forming galaxies at z$\sim$2

Many of the stars in today's galaxies formed during the peak epoch of star formation in the universe, which occured over the redshift range $2 \leq z \leq 4$ (Shapley, 2011). Outflows are present in many galaxies from $z \simeq 2-3$ (Shapley et al., 2003; Steidel et al., 2010). To study the behaviors of outflows, it is beneficial to study galaxies in these redshift ranges. The purpose of this project is to compare outflow velocities measured from absorption lines with the sizes and intensities of emission from star-forming regions measured with the Hubble Space Telescope. To do this, we draw our targets from the Keck Baryonic Structure Survey (KBSS), a spectroscopic survey of $\sim$2000 galaxies at z$\sim$2.

Instead of using a slit to obtain spectra, the Wide Field Camera 3 (WFC3) on the Hubble Space Telescope (HST) is able to disperse the entire field to create spectra of each object in the field of view. The F140W filter was used, which has a detection center at 1392.3nm with a Full Width Half Max (FWHM) width of 384nm. The G141 grism was also used, and it has a useful range of 1075-1700nm. After one orbit per field, it will have gathered the spectra for each object. It then repeats this process, but observing the field at a different angle. By combining each of these results, contamination from nearby objects can be minimized.

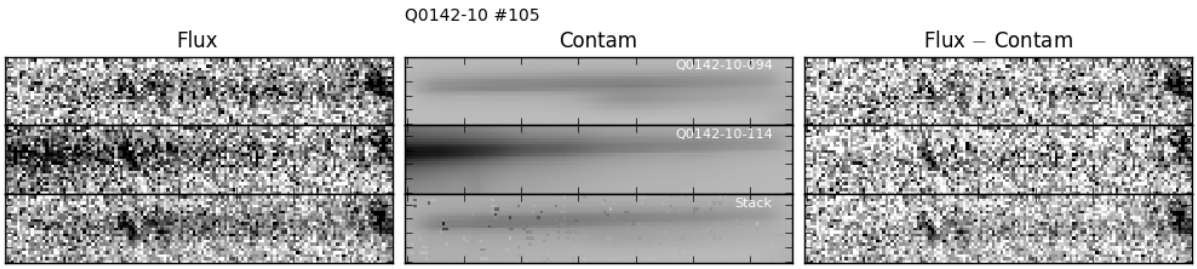

Figure 1.1: The x-axis represents the wavelength of light observed, and the y-axis is a spatial dimension. The left 3 images show the initial grism spectra for object BX165 in the Q0142-10 field of the KBSS. The middle column shows the calculated contamination from overlapping spectra of other objects in the field. The right column has the contamination removed from the spectra. The dark region on the right hand side of the spectrum is an [OIII] emission line.

The resulting spectrum of each object is very low resolution ($\sim$130 nm for the G141 grism), which prevents precise calculations from being made, such as the resolution of closely-spaced lines. However, due to the low spectral resolution combined with the high spatial resolution, emission line maps are able to be created. Figure 1.1 shows an example of a grism spectrum, and Figure 1.2 is an exmaple of the emission maps for the same object. The [OIII] $\lambda\lambda$4959, 5007 doublet is bright and can be seen on the right hand side of the spectrum as a large dark spot. At this resolution however, the individual lines cannot be resolved.

The goal of this project was to determine if there exists a correlation between the luminosity surface density of [OIII] emission and the outflow velocity of the galaxy. The [OIII] emission is a strong emission line arising in star-forming regions, and galaxies with a higher surface density of star formation are likely to also have a higher [OIII] luminosity density. Therefore, if there exists a correlation between [OIII] luminosity surface density and outflow velocity, then there most likely exists a correlation between SFR per area and outflow velocity. This would support the conclusion made by Heckman et al. (2015) that $v_{out} \propto SFR/area$. We expect that if this correlation exists, it is because the young, bright stars produce so much light, that they push away the surrounding gas. Since these massive stars are concentrated

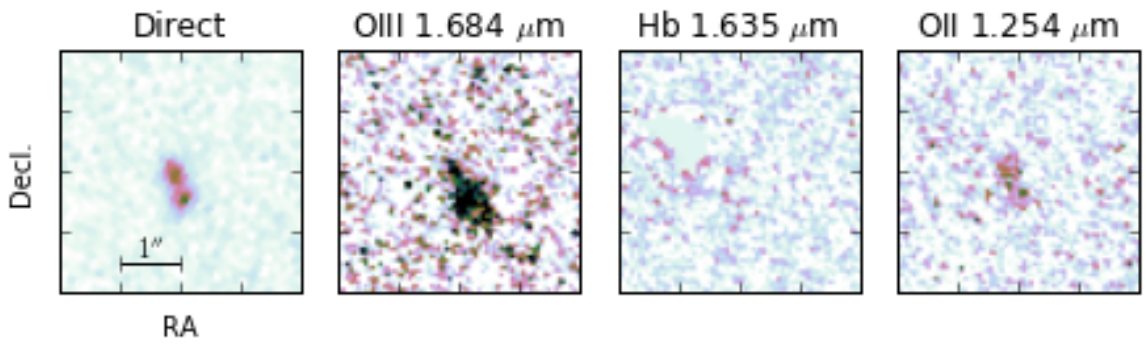

Figure 1.2: These are the emission line maps for object BX165 in the Q0142-10 field of the KBSS. The left image shows the total flux distribution over the specified area. Each subsequent picture shows the flux distribution at the observed wavelength. The wavelength shown represents the observed value, not the emitted.

in a small region, then with enough star formation, and therefore enough young, bright stars, this should drive galactic-scale outflows.

Section 2 will discuss what data was used and how it was filtered. Further, it will lay out how the data was analyzed. Section 3 will describe the conclusions and how they were determined.

Chapter 2

Sample Selection and Data

2.1 Sample Selection

The Keck Baryonic Structure Survey is a spectroscopic survey of ∼2000 galaxies in 15 different fields of view, at z∼2. At high redshifts, nearly all galaxies have large-scale outflows, therefore each galaxy in the KBSS will most likely be able to provide data on galactic outflows.

The KBSS has nebular redshifts and absorption redshifts for many of the objects in the survey. The nebular redshift is the redshift of the ionized gas, and the absorption redshift represents the redshift of the interstellar gas in the foreground of the galaxy after undergoing a Doppler shift. For objects with both redshifts available, the outflow velocity of the gas can be determined.

Grism data from the 3D-HST survey was available for 1509 of the objects in the 15 KBSS fields, an example of which is shown in Figure 1.1. Each spectrum was examined for prominent emission lines. Objects with spectra without prominent emission lines were ignored. Objects without a nebular redshift or absorption redshift were also ignored, so that outflow velocities could be determined for each remaining galaxy.

2.2 Data

Grism data from the 3D-HST survey for objects in the 15 KBSS fields was run through Gabriel Brammer's Grizli reduction[1], which is a piece of software designed for reducing data from slitless grism spectra. The reduction took in raw data files, and produced reprocessed images of the field, such as the reduced science images, an example of which can be seen in Figure 2.1, and dispersed images of the fields, an example of which is shown in Figure 2.2. The Grizli Reduction separated out each spectrum, and attempted to account for the flux from any overlapping spectra. It then output the contamination subtracted spectra for each object. An example of the grism spectrum after the Grizli reduction is shown in Figure 2.3.

After the reduction was run, the objects were filtered such that the only galaxies remaining were the same galaxies that had been previously selected for having nebular and absorption redshifts. These objects were run through a final step in the Grizli Reduction to create their emission line maps, similar to what was seen in Figure 1.2. These galaxies were then filtered further for objects with 3σ detections of [OIII] emission. After filtering for these criteria, 52 galaxies remained. The distribution of redshifts among the objects chosen is shown in Figure 2.4.

A program called Source Extractor is able to take an image of a portion of sky, determine the boundaries of the objects in the field, and calculate different physical properties such as size and total flux of each object. This program was run on each of the 52 emission line maps to determine the total isophotal area of the [OIII] flux. The distribution of areas of [OIII] emission can be seen in Figure 2.5. The [OIII] fluxes produced from the Grizli Reduction were used to calculate the [OIII] luminosities, and subsequently, the [OIII] luminosity/area values. These were then plotted against the corresponding outflow velocities calculated from the redshifts to determine if there

[1]The ReadMe and other documentation for Grizli can be found at `https://github.com/gbrammer/grizli`

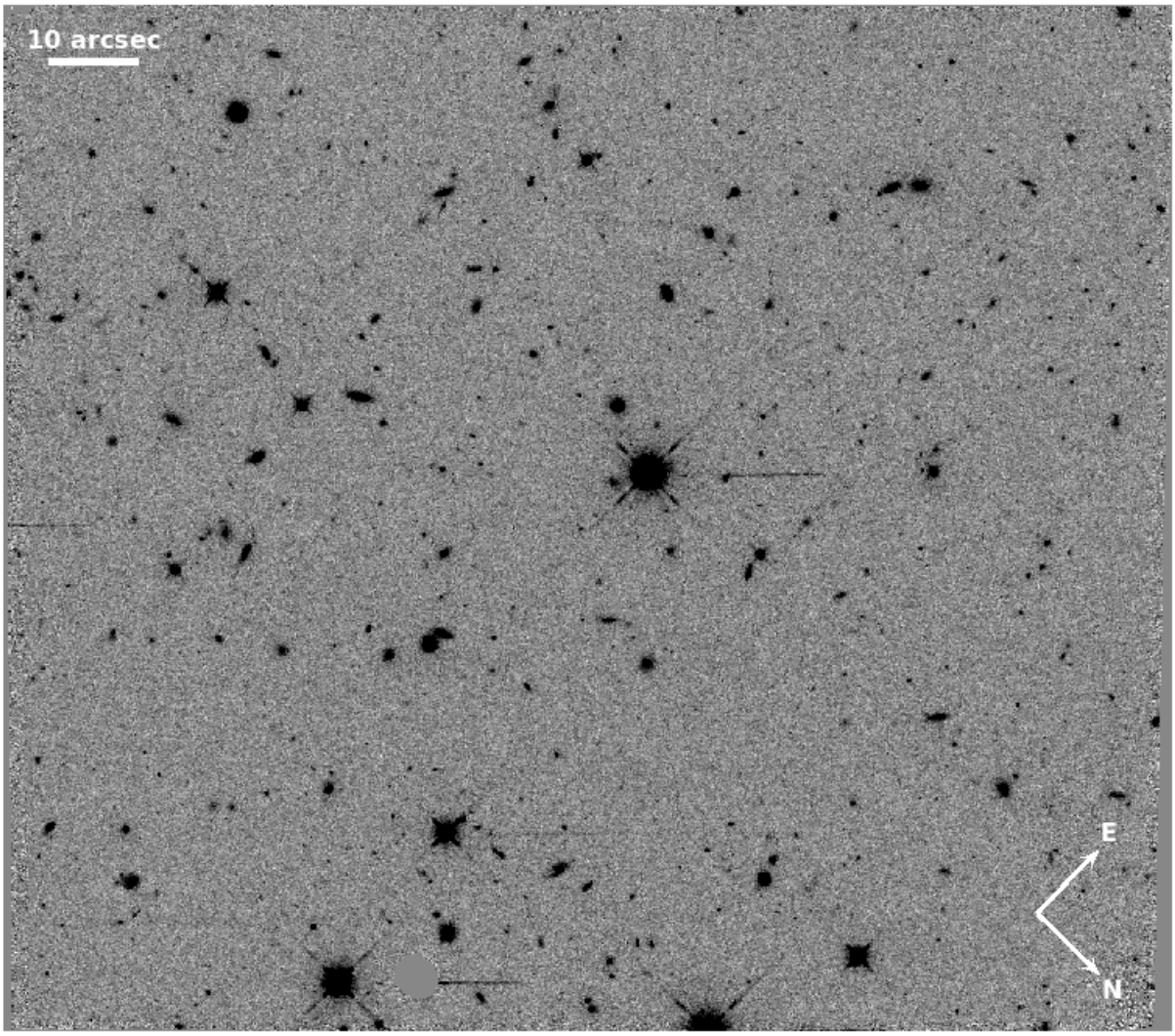

Figure 2.1: The direct F140W image of the Q1603 field.

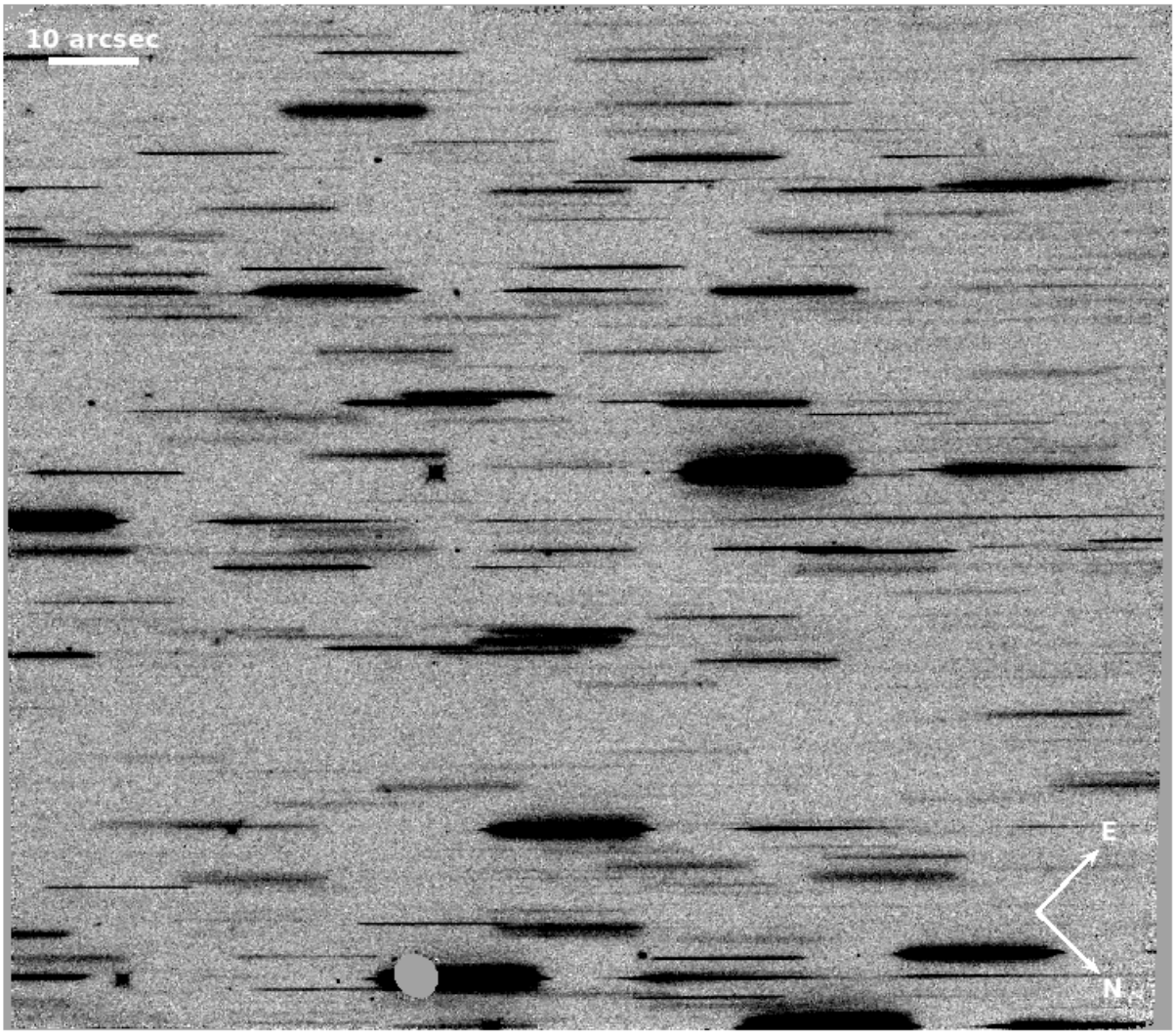

Figure 2.2: The dispersed G141 image of the Q1603 field.

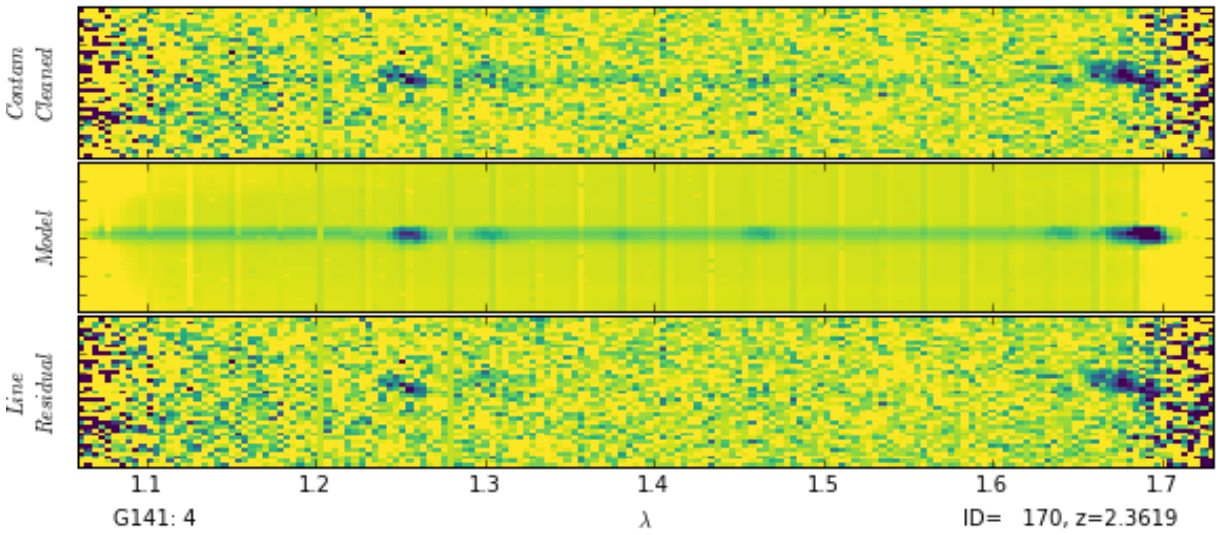

Figure 2.3: Grism spectra from the Grizli Reduction for object BX165 in the Q0142-10 field of the KBSS. The x-axis is in units of μm.

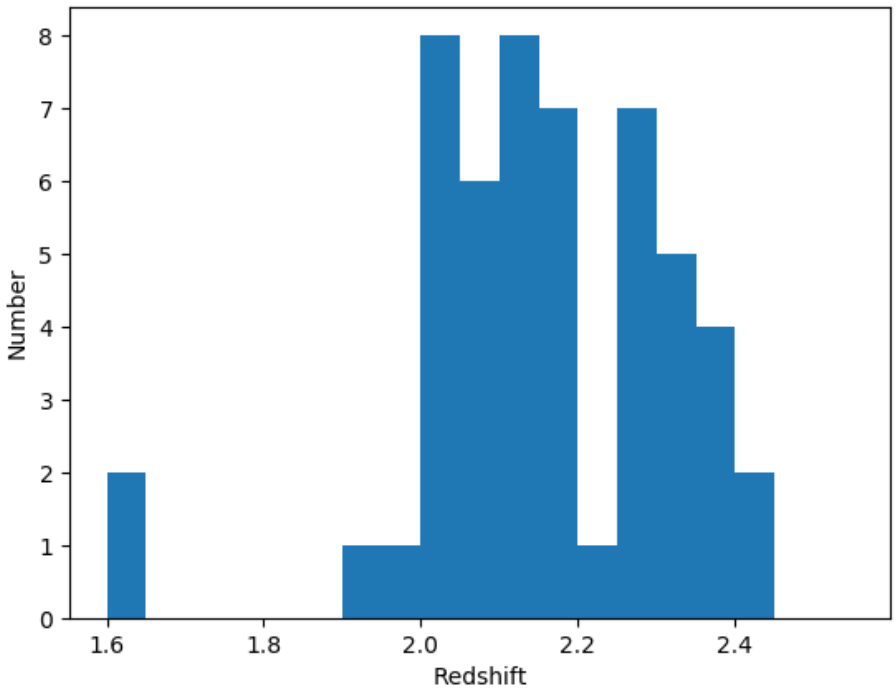

Figure 2.4: Distribution of nebular redshift values among the final galaxies chosen.

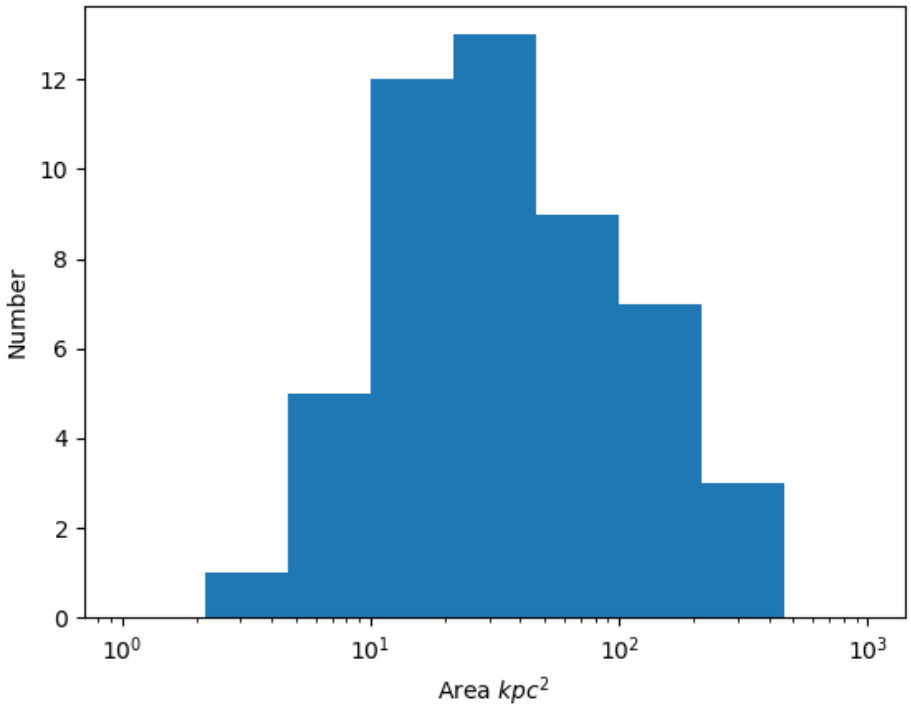

Figure 2.5: Distribution of galactic [OIII] emission areas.

was a correlation.

Chapter 3

Measurements and Conclusions

3.1 Measurements

When the luminosity surface density of [OIII] emission was plotted against the galactic outflow velocity, the result is seen in Figure 3.1. In determining if the data were correlated, a Spearman correlation coefficient of 0.055 was found, with a significance of 0.4σ. From this it can be concluded that according to this data, the luminosity surface density of [OIII] emission is not correlated with the galactic outflow velocity. It was also found that 12 of the 52 galaxies ($\approx$23%) had outflow velocities of 0 km s^{-1}. Additionally, there were 4 galaxies ($\approx$7.7%) that had negative outflow velocities, indicating that the gas was falling back onto the galaxy. If we ignore these 16 points where the calculated outflow velocity was $\leq$0 km s^{-1}, we find a Spearman correlation coefficient of 0.14, with a significance of 0.9σ. This indicates that according to our data, when only looking at true outflows, the luminosity surface density of [OIII] emission is not correlated with the galactic outflow velocity.

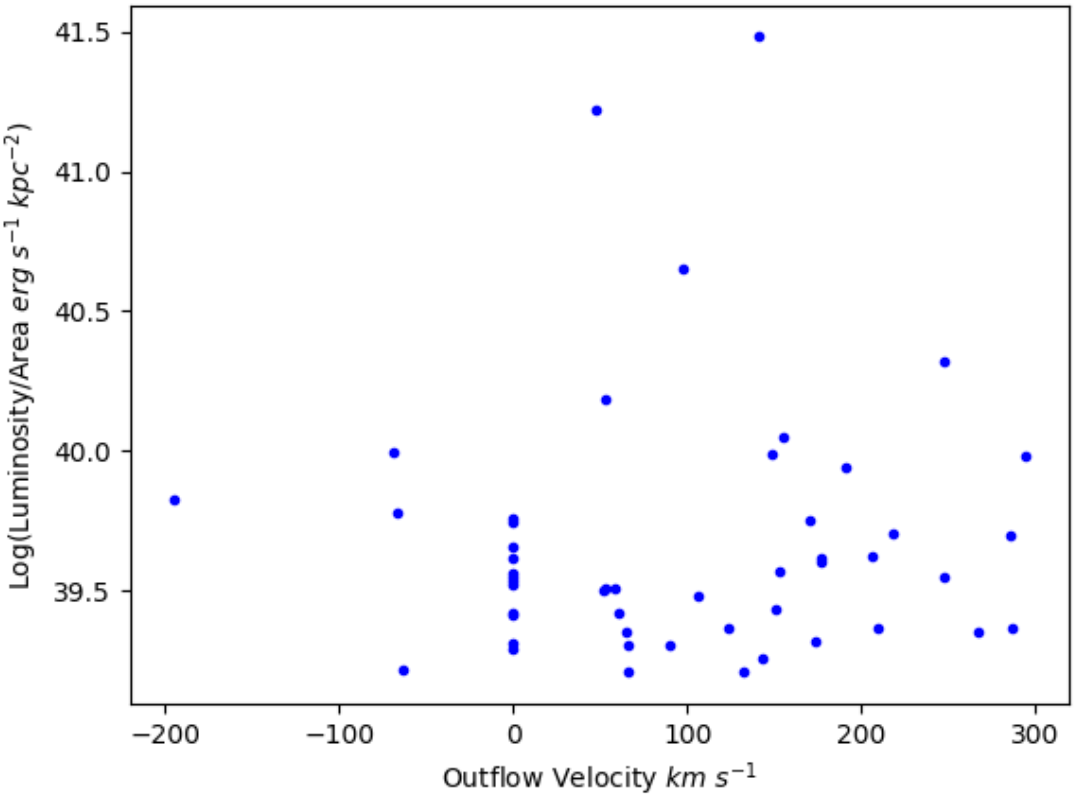

Figure 3.1: For the 52 galaxies sampled, there is a correlation significance of 0.4σ for the Log of the [OIII] luminosity surface density and the velocity of the galactic outflow. When ignoring points with calculated outflow velocities $\leq$0 km s^{-1}, the data has a correlation significance of 0.9σ. We can conclude from this that they do not seem to be correlated with one another.

3.2 Conclusions

Some of the galaxies have zero, or negative outflow velocities. Of the 52 galaxies sampled, 4 (≈7.7%) of them have calculated outflow velocities that are less than 0 km s^{-}1. This implies that the gas is not leaving the galaxy, but rather falling back onto it. There were also 12 (≈23%) galaxies that had outflow velocities of 0 km s^{-1}. It is possible these galaxies do not have enough radiation pressure to properly expel the gas, or they might have outflows that are collimated and pointing away from us.

We did not find any correlation between the luminosity per unit area of [OIII] emission compared to the galactic outlflow velocity. Since [OIII] emission is correlated with SFR, this implies that SFR/area is not proportional to v_{out}. This result disagrees with the findings of Heckman et al. (2015), which suggests a correlation between SFR/area and v_{out}. This disagreement could be due to the fact that [OIII] emission was used as an analog to SFR, instead of directly calculating it. Using Hα emission would allow for a more direct calculation of the SFR, and a larger sample size would allow for a wider range of galaxy properties to be examined. These additions could shed more light on the reasoning for the difference in findings.

Galactic outflows play a critical role in galaxy evolution. They bring gas content to higher radii in the galaxy which allows it to grow outwards. In doing so it also slows SFR near the center, causing active star formation to cease at smaller radii. Eventually this gas can be completely expelled from the galaxy, causing the injection of metals into the IGM. By understanding the relationship between SFR and outflow velocity, we can understand how current SFR can affect future SFR elsewhere in the galaxy.

Bibliography

Chevalier, R. A. & Clegg, A. W. 1985, Nature, 317, 44

Heckman, T. M. 2002, in Astronomical Society of the Pacific Conference Series, Vol. 254, Extragalactic Gas at Low Redshift, ed. J. S. Mulchaey & J. T. Stocke, 292

Heckman, T. M., Alexandroff, R. M., Borthakur, S., Overzier, R., & Leitherer, C. 2015, The Astrophysical Journal, 809, 147

Hopkins, P. F., Quataert, E., & Murray, N. 2012, Monthly Notices of the Royal Astronomical Society, 421, 3522

Martin, C. L. 2005, The Astrophysical Journal, 621, 227

Martin, C. L., Shapley, A. E., Coil, A. L., Kornei, K. A., Bundy, K., Weiner, B. J., Noeske, K. G., & Schiminovich, D. 2012, The Astrophysical Journal, 760, 127

Murray, N., Mnard, B., & Thompson, T. A. 2011, The Astrophysical Journal, 735, 66

Murray, N., Quataert, E., & Thompson, T. A. 2005, The Astrophysical Journal, 618, 569

Nelson, E. J., van Dokkum, P. G., Brammer, G., Schreiber, N. F., Franx, M., Fumagalli, M., Patel, S., Rix, H.-W., Skelton, R. E., Bezanson, R., Cunha, E. D., Kriek, M., Labbe, I., Lundgren, B., Quadri, R., & Schmidt, K. B. 2012, The Astrophysical Journal Letters, 747, L28

Nelson, E. J., van Dokkum, P. G., Förster Schreiber, N. M., Franx, M., Brammer, G. B., Momcheva, I. G., Wuyts, S., Whitaker, K. E., Skelton, R. E., Fumagalli, M., Hayward, C. C., Kriek, M., Labbé, I., Leja, J., Rix, H.-W., Tacconi, L. J., van der Wel, A., van den Bosch, F. C., Oesch, P. A., Dickey, C., & Ulf Lange, J. 2016, ApJ, 828, 27

Shapley, A. E. 2011, Annual Review of Astronomy and Astrophysics, 49, 525

Shapley, A. E., Steidel, C. C., Pettini, M., & Adelberger, K. L. 2003, The Astrophysical Journal, 588, 65

Steidel, C. C., Erb, D. K., Shapley, A. E., Pettini, M., Reddy, N., Bogosavljevi, M., Rudie, G. C., & Rakic, O. 2010, The Astrophysical Journal, 717, 289